N-Acylglycine Amidation: Implications for the Biosynthesis of Fatty Acid Primary Amides[†]

Benjamin J. Wilcox,[‡] Kimberly J. Ritenour-Rodgers,[‡] Alexander S. Asser,[‡] Laura E. Baumgart,[‡] Megan A. Baumgart,[‡] Dale L. Boger,[§] Jodi L. DeBlassio,[‡] Mitchell A. deLong,[∥] Uta Glufke,[⊥] Matthias E. Henz,[⊥] Lawrence King III,[‡] Kathleen A. Merkler,[‡] Jean E. Patterson,[§] John J. Robleski,[‡] John C. Vederas,[⊥] and David J. Merkler*[,‡]

Department of Chemistry and Biochemistry, Duquesne University, Pittsburgh, Pennsylvania 15282, Procter & Gamble Pharmaceuticals, Health Care Research Center, 8700 Mason−Montgomery Road, Mason, Ohio 45040, Department of Chemistry, The Scripps Research Institute, 10550 North Torrey Pines Road, La Jolla, California 92037, and Department of Chemistry, University of Alberta, Edmonton, Alberta, Canada T6G 2G2

Received September 18, 1998

ABSTRACT: Bifunctional peptidylglycine α-amidating enzyme (α-AE) catalyzes the O_2-dependent conversion of C-terminal glycine-extended prohormones to the active, C-terminal α-amidated peptide and glyoxylate. We show that α-AE will also catalyze the oxidative cleavage of *N*-acylglycines, from *N*-formylglycine to *N*-arachidonoylglycine. *N*-Formylglycine is the smallest amide substrate yet reported for α-AE. The $(V/K)_{app}$ for *N*-acylglycine amidation varies ∼1000-fold, with the $(V/K)_{app}$ increasing as the acyl chain length increases. This effect is largely an effect on the $K_{M,app}$; the $K_{M,app}$ for *N*-formylglycine is 23 ± 0.88 mM, while the $K_{M,app}$ for *N*-lauroylglycine and longer chain *N*-acylglycines is in the range of 60−90 μM. For the amidation of *N*-acetylglycine, *N*-(*tert*-butoxycarbonyl)glycine, *N*-hexanoylglycine, and *N*-oleoylglycine, the rate of O_2 consumption *is faster* than the rate of glyoxylate production. These results indicate that there must be the initial formation of an oxidized intermediate from the *N*-acylglycine before glyoxylate is produced. The intermediate is shown to be *N*-acyl-α-hydroxyglycine by two-dimensional $^1H-^{13}C$ heteronuclear multiple quantum coherence (HMQC) NMR.

Fatty acid primary amides represent a novel family of potent, bioactive lipids in humans and other mammals (*1*, *2*). Oleamide (*cis*-9-octadecenamide) induces sleep (*3*, *4*), blocks gap junction communication in glial cells (*5*, *6*), modulates serotonergic signal transduction (*7*−*9*), inhibits synovial fluid phospholipase A_2 (*10*), causes the same behavioral effects in mice as Δ^9-tetrahydrocannabinol and anandamide (*11*), and potentiates the antiproliferative effects of arachidonoylethanolamide in breast cancer cells (*12*). Erucamide (*cis*-13-docosenamide) stimulates the growth of blood vessels (*13*, *14*). In addition, Arafat et al. (*15*) characterized five long-chain fatty acid amides, palmitamide, palmitoleamide, oleamide, elaidamide, and linoleamide, from the luteal phase of human plasma. The biological roles of palmitamide, palmitoleamide, elaidamide, and linoleamide are unknown.

An understanding of the pathways by which the fatty acid primary amides are produced and degraded in vivo is critical to establishing their physiological roles and to controlling diseases that result from defects in their anabolism and catabolism. A specific fatty acid amide hydrolase is responsible for their degradation (*16*−*19*). The pathway for the biosynthesis of these novel amidated lipids is not currently understood. Merkler et al. (*20*) showed that bifunctional peptidylglycine α-amidating enzyme (α-AE,[1] EC 1.14.17.3) cleaved *N*-myristoylglycine to myristamide. The *N*-acylglycines are produced in vivo from the fatty acyl-CoA thioesters and glycine by acyl-CoA:glycine *N*-acyltransferase (ACGNAT, EC 2.3.1.13) (*21*, *22*). The sequential actions of ACGNAT and α-AE could lead to the production of a wide variety of fatty acid primary amides (Scheme 1).

Most mammalian and insect peptide hormones possess a C-terminal α-amide moiety (*23*−*25*) that arises from the oxidative cleavage of the C-terminal glycyl $C_\alpha-N$ bond in a glycine-extended peptide precursor (*26*, *27*). The enzyme that catalyzes the posttranslational amidation reaction is α-AE, a bifunctional, copper- and zinc-dependent monooxy-

[†] Supported by grants from the Human Growth Foundation, Hunkele Foundation, Whitehall Foundation, and the Duquesne University Faculty Development Fund to D.J.M., an operating grant from the Natural Sciences and Engineering Research Council of Canada to J.C.V., and the National Institutes of Health (CA 42056) to D.L.B. Postdoctoral fellowships to U.G. from Deutsche Forschungsgemeindschaft and to M.E.H. from the Swiss National Science Foundation are gratefully acknowledged. B.J.W. was supported by a summer undergraduate research fellowship from Bayer Corporation. L.E.B. and J.L.D. were supported by summer research fellowships from the Duquesne University Undergraduate Research Program.

* To whom correspondence should be addressed: FAX: (412) 396-5683; e-mail merkler@duq3.cc.duq.edu.

[‡] Department of Chemistry and Biochemistry, Duquesne University.

[§] Department of Chemistry, The Scripps Research Institute.

[∥] Procter & Gamble.

[⊥] Department of Chemistry, University of Alberta.

[1] Abbreviations: Ac, acetyl; ACGNAT, acyl-CoA:glycine *N*-acyltransferase; α-AE, bifunctional peptidylglycine α-amidating monooxygenase; PAL, monofunctional peptidylamidoglycolate lyase; PHM, monofunctional peptidyl α-hydroxylating monooxygenase; tBOC, *tert*-butoxycarbonyl; TFA, trifluoroacetic acid.

10.1021/bi982255j CCC: $18.00
Published on Web 02/25/1999

Scheme 1: Proposed Pathway for the Biosynthesis of Fatty Acid Primary Amides

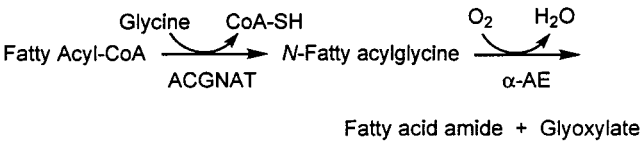

genase (*27*−*29*) that has structural and catalytic similarities to another copper-dependent monooxygenase, dopamine β-monooxygenase (*30*). The amidation of C-terminal glycine-extended peptides is a two-step reaction catalyzed by separate catalytic units. The first step, catalyzed by peptidyl α-hydroxylating monooxygenase (PHM), is the copper-, O_2-, and ascorbate-dependent hydroxylation of the α-carbon of the C-terminal glycine. The second step, catalyzed by peptidylamidoglycolate lyase (PAL), is the zinc-dependent dealkylation of the α-hydroxyglycine-extended peptide to the α-amidated peptide and glyoxylate (for a recent review on α-AE, see ref *31*). In mammals, numerous forms of the α-amidating enzyme are expressed, including bifunctional PAM and the monofunctional enzymes PHM and PAL (*32*−*34*). An alternatively spliced dibasic amino acid processing site is located between the PHM and PAL domains of bifunctional PAM (*34*−*36*). The presence of the dibasic processing site facilitates the proteolytic separation of PHM and PAL into individual catalytic units.

Previous studies of the substrate specificity have focused primarily on the amidation of peptides (*37*, *38*). Only a few studies have shown that α-AE will amidate non-peptide substrates (*39*, *40*), and these reports have been limited to a small number of compounds. We now report that α-AE will amidate a diversity of *N*-acylglycines from *N*-formylglycine to *N*-arachidonoylglycine. The *V*/*K* for acylglycine amidation increases as the acyl chain length increases, reaching a plateau value that is ∼4-fold higher than the *V*/*K* for D-Tyr-Val-Gly, a prototypical peptide substrate. This is the first report of biologically occurring, non-peptide substrates for α-AE with *V*/*K* values comparable to those for the best glycine-extended peptide substrates. In addition, we show that an intermediate *N*-acyl-α-hydroxyglycine is first formed from the *N*-acylglycine and is subsequently dealkylated to the acylamide and glyoxylate. Finally, we report that the nonfluorescent *N*-acylglycines inhibit the crude human serum α-AE-catalyzed conversion of *N*-dansyl-Tyr-Val-Gly to *N*-dansyl-Tyr-Val-NH_2 with K_i values that agree with the K_M values determined with purified rat α-AE. These results provide further evidence that α-AE could have a role in the biosynthesis of fatty acid primary amides and represent a lead for the development of novel nonpeptidic inhibitors of this enzyme. α-AE inhibitors could be clinically useful in controlling the acute inflammatory response (*41*) and in treating lung carcinoma (*42*).

MATERIALS AND METHODS

Materials. Glycylglycine, *N*-sarcosylglycine, β-Ala-Gly, *N*-(L-α-aminobutyryl)glycine, *N*-(chloroacetyl)glycine, *N*-acetyl-Gly-Gly, *N*-acetyl-Leu-Gly, and *N*-myristoylglycine were obtained from Bachem Biosciences; *N*-dansyl-Tyr-Val-Gly, D-Tyr-Val-Gly, hydantoic acid, sodium ascorbate, glyoxylic acid monohydrate, lactate dehydrogenase, and NADH were obtained from Sigma; tBOC-glycine, *N*-octanoylglycine, hippuric acid, and butyramide were obtained from Aldrich; *N*-acetylglycine, *N*-isovaleroylglycine, and *N*-tigloylglycine were obtained from TCI America; *N*-lauroylglycine and *N*-decanoylglycine were obtained from Novabiochem; *N*-carboxyglycine and *N*-[(D,L)-α-bromoisovaleroyl]glycine were obtained from Pfaltz & Bauer; 5-butylhyantoic acid was obtained from ACROS; *N*-(trifluoroacetyl)glycine was obtained from Advanced ChemTech; *N*-(acetoacetyl)glycine was obtained from Lancaster; *N*-chloroacetyl-Gly-Gly was obtained from Research Organics; *N*-methoxycarbonylglycine was obtained from Senn Chemicals AG; [*glycyl*-1,2-$^{13}C_2$]-tBOC-glycine was obtained from Isotech; and bovine catalase was obtained from Worthington. Human serum was obtained from whole blood drawn from a healthy 22 year old female volunteer by venipuncture. Blood was allowed to clot and the serum was collected by centrifugation. Serum was frozen and stored at −70 °C until use. (*R*,*S*)-*N*-Butyryl-α-hydroxyglycine was synthesized from glyoxylate and butyramide as described (*43*). *N*-Oleoylethanolamide was synthesized according to the procedure of Roe et al. (*44*). All other reagents were of the highest quality available commercially.

Chemical Syntheses of N-Acylglycines and N-Ac-Phe-Pyruvate. The synthesis of *N*-Ac-Phe-pyruvate was done as described in the literature (*45*) but with a modified hydrolysis procedure, as described in the Supporting Information. The syntheses of *N*-propionylglycine, *N*-(D,L)-α-methylbutyrylglycine, and *N*-hexanoylglycine employed a procedure very similar to the following one used to make *N*-butyrylglycine. Full details and spectra for these compounds are given in the Supporting Information. Butyric anhydride (1.1 mL, 6.7 mmol) was added to a solution of glycine (0.5 g, 6.7 mmol) in 2 M aqueous sodium hydroxide (4 mL, 8.0 mmol) at 0 °C. The reaction mixture was stirred 3 h at room temperature. During this time 2 M aqueous sodium hydroxide (3 mL, 6.0 mmol) was added to keep the pH at 8. The reaction mixture was then acidified and extracted with ethyl acetate (4 × 20 mL). The combined organic layers were washed with brine (15 mL), dried over $MgSO_4$, and evaporated *in vacuo* to give *N*-butyrylglycine (0.8 g, 84%). Recrystallization from ethyl acetate/petrol ether (40−60 °C) afforded 0.6 g (64%) of pure product as white crystals: mp 76−78 °C, lit. mp 68.5−70 °C (*46*).

N-Oleoylglycine was synthesized as follows. Oleic acid (100 μL, 0.32 mmol), glycine ethyl ester hydrochloride (46 mg, 0.33 mmol), anhydrous triethylamine (66 μL, 0.47 mmol), and anhydrous methylene chloride (5 mL) were combined under an N_2 atmosphere and cooled to 0 °C. EDCI (107 mg, 0.56 mmol) and DMAP (8 mg, 0.07 mmol) were added and the reaction was allowed to stir at 25 °C for 4 h. The solvent was removed under reduced pressure and the crude product was chromatographed (SiO_2, 2 × 15 cm, 20−33% ethyl acetate−hexane gradient elution) to afford the ethyl ester (110 mg, 94%) as a white solid, mp 32−33 °C. The ethyl ester (726 mg, 1.97 mmol) was dissolved in 6 mL of THF/CH_3OH/H_2O (3:1:1). The solution was treated with $LiOH·H_2O$ (237 mg, 5.63 mmol) and stirred at 25 °C for 15 min. The solution was diluted with 1 N HCl (30 mL) and extracted with ethyl acetate (3 × 30 mL). The combined organic layers were dried over Na_2SO_4, and concentrated under reduced pressure to afford *N*-oleoylglycine (611 mg, 91%) as a white solid, mp 90−91 °C. Full details and spectra

for *N*-oleoylglycine and the ethyl ester are given in the Supporting Information.

N-Linolenoylglycine and *N*-arachidonoylglycine were synthesized by similar procedures as follows. A suspension of glycine methyl ester hydrochloride (235 mg, 1.87 mmol) and *N*,*N*-diisopropylethylamine (313 μL, 1.80 mmol) in dichloromethane (6 mL) was added to a solution of linolenic acid (438 μL, 1.44 mmol), benzotriazol-1-yloxy-tris(pyrrolidino)-phosphonium hexafluorophosphate (972 mg, 1.87 mmol) and *N*,*N*-diisopropylethylamine (313 μL, 1.80 mmol) in dichloromethane (10 mL). The reaction mixture was stirred for 3.5 h at room temperature, under argon in the dark. The reaction mixture was then diluted with dichloromethane (20 mL) and washed with brine (3 × 15 mL), 2 M hydrochloric acid (3 × 15 mL), saturated sodium hydrogen carbonate (3 × 15 mL), and brine (2 × 15 mL). The organic layer was dried over $MgSO_4$ and evaporated in vacuo. Purification by column chromatography [silica gel, petrol ether (40−60 °C)/ethyl acetate 5/2] yielded *N*-linolenylglycine methyl ester (473 mg, 94%) as a yellow oil. A solution of this methyl ester (250 mg, 0.72 mmol) in tetrahydrofuran (2.4 mL) was treated with 1 M aqueous lithium hydroxide (787 μL, 0.79 mmol). After 45 min of stirring under argon, at room temperature, the main part of the solvent was evaporated in vacuo. The residue was diluted with water (15 mL), acidified to pH 3.0 with 2 M hydrochloric acid (color of the solution changed from yellow to colorless), and extracted with ethyl acetate (3 × 20 mL). The combined organic layers were washed with water (2 × 20 mL), dried over $MgSO_4$, and evaporated in vacuo. Purification by RP-HPLC [resolve-C18, water (0.1% TFA)/acetonitrile (0.1% TFA) 75/25 → 0/100) yielded *N*-linolenylglycine (231 mg, 96%) as a white solid, mp 61−63 °C (chloroform/hexane). Full details and spectra for *N*-linolenoylglycine, *N*-arachidonoylglycine, and their methyl esters are given in the Supporting Information.

Initial Rate Studies. Reactions at 37.0 ± 0.1 °C were initiated by the addition of α-AE (10−50 μg) into 2.4 mL of 100 mM MES/NaOH, pH 6.0, 30 mM NaCl, 1% (v/v) ethanol, 0.001% (v/v) Triton X-100, 1.0 μM $Cu(NO_3)_2$, 5.0 mM sodium ascorbate, and *N*-acylglycine (generally 0.2−3.0$K_{M,app}$). The final α-AE concentration ranged from 56 to 280 nM based on a molecular mass of 75 kDa for the bifunctional protein. Initial rates were measured by following the α-AE-dependent consumption of O_2 on a Yellow Springs Instrument Model 53 oxygen monitor. V_M values were normalized to controls performed at 11.0 mM *N*-acetylglycine. Ethanol was added to protect the catalase against ascorbate-mediated inactivation (*47*) and Triton X-100 was included to prevent nonspecific absorption of the enzyme to the sides of the oxygen monitor chambers.

Peptidylglycine α-Amidating Enzyme. Chinese hamster ovary cells that secrete recombinant type A rat medullary thyroid carcinoma α-AE into the culture medium (*35*) were grown in a Cellco Cellmax-100 hollow fiber bioreactor (*48*). The bifunctional enzyme was purified as described by Miller et al. (*49*) except that the final gel-filtration step (Sephacryl S-300) was carried out in 20 mM HEPES/NaOH, pH 7.8, 50 mM NaCl, and 0.001% (v/v) Triton X-100. The amidation of *N*-dansyl-Tyr-Val-Gly to *N*-dansyl-Tyr-Val-NH_2 (*50*) was used throughout the enzyme purification to screen column fractions. Unless noted, the α-AE used in these studies had a specific activity ≥ 3.0 μmol of O_2 consumed min^{-1} mg^{-1} at 37 °C under standard conditions. Standard conditions were 100 mM MES/NaOH, pH 6.0, 30 mM NaCl, 1% (v/v) ethanol, 0.001% (v/v) Triton X-100, 10 μg/mL bovine catalase, 1.0 μM $Cu(NO_3)_2$, 5.0 mM sodium ascorbate, and 11.0 mM *N*-acetylglycine.

Glyoxylate Determination. Glyoxylate was determined by the spectrophotometric method of Christman et al. (*51*) as modified by Katopodis and May (*40*). Under acidic conditions, glyoxylate is oxidized to the red-colored 1,5-diphenylformazan in the presence of excess phenylhydrazine and ferricyanide (*52*). Standard curves of [glyoxylate] vs A_{520} were constructed in the appropriate buffers by using a glyoxylate solution that had been calibrated by measuring the glyoxylate-dependent oxidation of NADH ($\Delta\epsilon_{340} = 6.22 \times 10^3$ M^{-1} cm^{-1}) as catalyzed by lactate dehydrogenase.

Reverse-Phase HPLC Assay of N-Butyrylglycine Amidation. HPLC assays were performed with a Hewlett-Packard 1090 liquid chromatograph equipped with a binary solvent delivery system, a heated column compartment, an autosampler, and an autoinjector. Separations were achieved on a Phenomenex Luna C_{18} column (250 × 4.6 mm; 5 μm particles) fitted with a Brownlee RP-18 guard column. The substrate, *N*-butyrylglycine, the carbinolamide intermediate, (*S*)-*N*-butyryl-α-hydroxyglycine, and amidated product, butyramide, were resolved at 50 °C by isocratic elution with a mobile phase of 2.5 mM ammonium phosphate, pH 2.5/acetonitrile (97.6/2.4). Analytes were detected at 214 nm using a Hewlett-Packard Model 79853A variable-wavelength detector.

Isolation of Enzymatically Produced N-Hexanoyl-α-hydroxyglycine. Reactions were initiated by the addition of rat α-AE (1.0 mg, 13 nmol) to 10 mL of 10 mM MES/NaOH, pH 6.0, 4.0 mM NaCl, 6.0 mM sodium ascorbate, 1.0 μM $Cu(NO_3)_2$, 10 μg/mL catalase, 100 μM *N*-Ac-Phe-pyruvate, and 5.0 mM *N*-hexanoylglycine. After a 6 h incubation at 37 °C, the enzyme was removed by diafiltration through a Centricon-30 filter. Separations were achieved on a Vydac C_{18} column (250 × 4.6 mm; 5 μm particles) fitted with a Waters μBondapak C_{18} guard column. *N*-Hexanoylglycine and *N*-hexanoyl-α-hydroxyglycine were resolved by a linear gradient of 2.5 mM ammonium phosphate, pH 2.5, to 2.5 mM ammonium phosphate/acetonitrile (80/20) over 30 min. Analytes were detected at 218 nm using a Bio-Rad Model 1305A UV detector. Mass spectra of the *N*-hexanoyl-α-hydroxyglycine were obtained with a Micromass ZabSpec mass spectrometer using electrospray ionization with the sample dissolved in water/acetonitrile.

NMR Spectroscopy. The two-dimensional $^1H-^{13}C$ heteronuclear multiple quantum coherence spectra (HMQC) were obtained using a Varian INOVA 600 spectrometer at 27 °C and referenced to acetone as an external standard, which puts the HOD signal to 4.75 ppm. A sweep width of 4000 Hz with 6464 data points was used to define the ^1H spectrum, and 256 data points were used to define 7543 Hz in the ^{13}C dimension.

Inhibition of Human Serum α-AE. Reactions were carried out at 37 °C in 50 mM HEPES/NaOH, pH 7.4, 1.2 mM sodium ascorbate, 10 μM $Cu(NO_3)_2$, 4.0 μM *N*-dansyl-Tyr-Val-Gly, 60 μg/mL catalase, 6.1 mg/mL human plasma, and the *N*-acylglycine (0.4−3.0 K_i). Amidation of *N*-dansyl-Tyr-Val-Gly was monitored by HPLC.

Data Analysis. Kinetic parameters for linear double-reciprocal plots were fit to

$$v = (V_{M,app}[A])/(K_{M,app} + [A]) \quad (1)$$

where $K_{M,app}$ is the apparent Michaelis constant for the *N*-acylglycine, A, at constant fixed concentrations of ascorbate and O_2 and $V_{M,app}$ is the apparent catalytic rate at saturating [A] under the conditions of the experiment (*53*). Values for $K_{i,s}$ were obtained from Dixon analysis at a constant substrate concentration:

$$\frac{V_{m,app}}{v} = 1 + \frac{K_{M,app}}{[A]}\left(1 + \frac{[I]}{K_{i,s}}\right) \quad (2)$$

Data obtained upon the amidation of an *N*-acylglycine for the decrease of $[O_2]$ vs time and the increase in [glyoxylate] vs time were fit to a scheme consisting of two consecutive, irreversible first-order steps:

$$O_2 \xrightarrow{k_1} \text{intermediate} \xrightarrow{k_2} \text{glyoxylate} \quad (3)$$

The concentration of O_2 at time = *t*, $[O_2]_t$, was analyzed according to

$$[O_2]_t = [O_2]_0 e^{-k_1 t} + [O_2]_\infty \quad (4)$$

where $[O_2]_\infty$ is the concentration of O_2 at infinite time[2] and $[O_2]_0$ is the initial concentration of O_2; $[O_2]_0 = 200$ μM at 37 °C (*54*). A value for k_1 (± standard error) was obtained by a nonlinear regression fit of the data for the $[O_2]$ vs time by Sigma Plot. The concentration of O_2 consumed at time = *t*, $[O_2]_{consumed,t}$, was obtained from

$$[O_2]_{consumed,t} = [O_2]_0 - [O_2]_t \quad (5)$$

The concentration of glyoxylate at time = *t*, $[glyoxylate]_t$, was analyzed according to

$$[\text{glyoxylate}]_t = [\text{acyl-Gly}]_0\left(1 - \frac{k_2 e^{-k_1 t}}{k_2 - k_1} + \frac{k_1 e^{-k_2 t}}{k_2 - k_1}\right) \quad (6)$$

where $[acyl\text{-}Gly]_0$ is the initial concentration of the *N*-acylglycine. A value for k_2 (± standard error) was obtained by a nonlinear regression fit of the data for [glyoxylate] vs time using Sigma Plot with the value of k_1 fixed at that obtained from the $[O_2]$ vs time data.

RESULTS

Amidation of N-(Fatty acyl)glycines. Merkler et al. (*20*) first reported that recombinant rat α-AE catalyzed the amidation of *N*-myristoylglycine to myristamide. As presented in Tables 1 and 2, we have found that α-AE will amidate a diversity of *N*-acylglycines. The long-chain *N*-(fatty acyl)glycines have limited aqueous solubility. In our experience, *N*-lauroylglycine is the *N*-acylglycine with the longest acyl chain that could be prepared as a 5−10 mM aqueous solution. The amidation of *N*-(fatty acyl)glycines with acyl chains of ≥13 carbon atoms required the addition of an organic cosolvent, 2.5% (v/v) DMSO, to solubilize the long-chain *N*-(fatty acyl)glycines at concentrations ≤300 μM. The amidation of long-chain *N*-(fatty acyl)glycines in 2.5% (v/v) DMSO is shown in Table 2. *N*-Arachidonoylglycine is also amidated by α-AE. Due to the substrate inhibition at concentrations >25 μM, it was not possible to measure the kinetic constants for *N*-arachidonoylglycine. The initial rate of O_2 consumption decreased from 3.6 ± 0.62 μmol min^{-1} mg^{-1} at 25 μM *N*-arachidonoylglycine to 2.7 ± 0.09 μmol min^{-1} mg^{-1} at 63 μM *N*-arachidonoylglycine. In addition, we found no α-AE-dependent consumption of O_2 in the presence of *N*-carboxyglycine and *N*-oleoylethanolamine when they were tested from 0.05 to 1.0 mM. Further studies showed that *N*-oleoylethanolamine concentrations as high as 200 μM did not inhibit the α-AE catalyzed amidation of 5.0 mM *N*-acetylglycine (King and Merkler, unpublished results).

α-AE-Dependent Formation of Glyoxylate from N-Acylglycines. The data in Tables 1 and 2 show that there is an α-AE-dependent consumption of O_2 in the presence of the indicated *N*-acylglycines. These data do not prove that there has been cleavage at the α-carbon of the glycyl moiety to form the acylamide and glyoxylate. The formation of glyoxylate provides a general method to demonstrate the oxidative cleavage of any *N*-acylglycine. Glyoxylate production from 10 different *N*-acylglycines after a 3 h incubation in the presence of α-AE and ascorbate is shown in Figure 1. In each case, glyoxylate is produced, indicative of C_α−N bond cleavage. However, the total amount of glyoxylate produced varied from 31 ± 15 μM for *N*-formylglycine to 630 ± 63 μM for *N*-lauroylglycine. The data in Figure 1 correlate well with the results presented in Table 1: the higher the $(V/K)_{app}$ for O_2 consumption, the higher the final concentration of glyoxylate formed after incubation with enzyme and ascorbate.

A comparison of the rate of glyoxylate production vs the rate of O_2 consumption for tBOC-glycine and *N*-hexanoylglycine is presented in Figure 2. For both tBOC-glycine and *N*-hexanoylglycine, the rate of O_2 consumption is greater than the rate of glyoxylate production. Similarly, the rate of O_2 consumption was greater than the rate of glyoxylate production for the amidation of *N*-acetylglycine and *N*-oleoylglycine (data not shown). This pattern of results indicates that there must be an initial formation of an oxidized intermediate from the *N*-acylglycine before glyoxylate is produced. Analogous to the work on the amidation of glycine-extended peptides (*55, 56*), this intermediate is postulated to be the carbinolamide, *N*-acyl-α-hydroxyglycine. The data in Figure 2A are also consistent with the *N*-Ac-Phe-pyruvate inhibition of only PAL: there is little effect on O_2 consumption and a significant decrease in the formation of glyoxylate (*45*).

Ideally, the progress curves obtained for O_2 consumption and glyoxylate production should be described by two consecutive, irreversible first-order steps (eq 3). The progress curves obtained for the amidation of 180 μM *N*-hexanoylglycine are reasonably fit using values of $k_1 = 0.83 \pm 0.01$ min^{-1} and $k_2 = 0.19 \pm 0.01$ min^{-1} (Figure 2B). For this experiment, $[N\text{-hexanoylglycine}]_{initial} < [O_2]_{initial}$ and was approximately equal to the final concentration of glyoxylate produced, $[N\text{-hexanoylglycine}]_{initial} \approx [glyoxylate]_{final}$. The progress curves obtained upon the incubation of enzyme with 1.8 mM tBOC-Gly or 5.0 mM *N*-acetylglycine could not be

[2] If $[O_2]_0 > [N\text{-acylglycine}]$, then $[O_2]_\infty = [O_2]_0 - [N\text{-acylglycine}]_0$. If $[N\text{-acylglycine}]_0 > [O_2]_0$, then $[O_2]_\infty = 0$.

Table 1: Comparison of K_M, V_M, and V_M/K_M Values for *N*-Acylglycines with Rat α-AE[a,b]

substrate	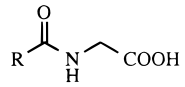	$K_{M,app}$ (mM)	$V_{M,app}$ (μmol min^{-1} mg^{-1})	relative $(V/K)_{app}$
hydantoic acid	R = NH_2	$(3.3 \pm 0.20) \times 10^1$	7.7 ± 0.24	0.33
Gly-Gly	R = NH_2CH_2	$(1.1 \pm 0.29) \times 10^1$	2.8 ± 0.43	0.36
N-(trifluoroacetyl)glycine	R = CF_3	4.1 ± 0.34	1.4 ± 0.057	0.50
N-formylglycine	R = H	$(2.3 \pm 0.88) \times 10^1$	8.7 ± 0.14	0.55
β-Ala-Gly	R = $NH_2CH_2CH_2$	6.6 ± 1.0	2.8 ± 0.15	0.62
N-acetylglycine	R = CH_3	9.3 ± 0.47	6.4 ± 0.15	1.0
N-sarcosylglycine	R = CH_3NHCH_2	5.8 ± 0.54	4.2 ± 0.20	1.1
γ-Glu-Gly-Gly	R = $NH_2CH(COOH)CH_2CH_2C(=O)NHCH_2$	2.1 ± 0.32	1.8 ± 0.097	1.2
N-(methoxycarbonyl)glycine	R = CH_3-O	6.5 ± 0.14	5.9 ± 0.051	1.3
N-(L-α-aminobutyryl)glycine	R = $CH_3CH_2CH(NH_2)$	6.2 ± 0.43	6.7 ± 0.19	1.6
N-valproylglycine	R = $(CH_3CH_2CH_2)_2CH$	3.0 ± 0.24	4.2 ± 0.17	2.0
N-(*tert*-butoxycarbonyl)glycine (tBOC-glycine)	R = $(CH_3)_3C-O$	3.7 ± 0.19	6.5 ± 0.15	2.6
N-tigloylglycine	R = $CH_3CH=C(CH_3)$	3.2 ± 0.20	6.2 ± 0.19	2.8
N-chloroacetylglycine	R = $ClCH_2$	2.0 ± 0.15	5.7 ± 0.12	4.1
N-propionoylglycine	R = CH_3CH_2	2.5 ± 0.22	8.6 ± 0.28	5.0
N-[(D,L)-α-methylbutyryl]glycine	R = $CH_3CH_2CH(CH_3)$	2.6 ± 0.13	9.5 ± 0.18	5.3
N-butyrylglycine	R = $CH_3CH_2CH_2$	2.0 ± 0.10	8.6 ± 0.13	6.2
N-isovaleroylglycine	R = $(CH_3)_2CHCH_2$	2.0 ± 0.13	8.8 ± 0.24	6.4
N-[(D,L)-α-bromoisovaleroyl]glycine	R = $(CH_3)_2CHCH(Br)$	1.5 ± 0.069	6.8 ± 0.10	6.6
N-acetyl-Gly-Gly	R = $CH_3C(=O)NHCH_2$	1.5 ± 0.073	7.1 ± 0.14	6.9
hippuric acid (*N*-benzoylglycine)	R = C_6H_5	1.3 ± 0.036	6.5 ± 0.064	7.3
5-butylhydantoic acid	R = $CH_3(CH_2)_3NH$	1.0 ± 0.089	8.0 ± 0.44	12
N-(acetoacetyl)glycine	R = $CH_3C(=O)CH_2$	0.64 ± 0.025	5.6 ± 0.10	13
N-chloroacetyl-Gly-Gly	R = $ClCH_2C(=O)NHCH_2$	0.50 ± 0.033	7.5 ± 0.18	22
N-hexanoylglycine	R = $CH_3(CH_2)_4$	0.42 ± 0.057	8.0 ± 0.28	28
D-Tyr-Val-Gly	R = D-Tyr-Val	0.22 ± 0.031	7.9 ± 0.78	52
N-octanoylglycine	R = $CH_3(CH_2)_6$	0.20 ± 0.0083	10.4 ± 0.17	76
N-acetyl-Leu-Gly	R = $CH_3C(=O)NHCH[CH_2CH(CH_3)_2]$	0.096 ± 0.0091	8.2 ± 0.36	124
N-decanoylglycine	R = $CH_3(CH_2)_8$	0.10 ± 0.0041	12.6 ± 0.19	183
N-lauroylglycine	R = $CH_3(CH_2)_{10}$	0.061 ± 0.0031	8.3 ± 0.17	188

[a] Reactions were carried out at 37 °C in 100 mM MES/NaOH, pH 6.0, 30 mM NaCl, 1.0% (v/v) ethanol, 0.001% (v/v) Triton X-100, 5.0 mM sodium ascorbate, 1.0 μM $Cu(NO_3)_2$, 10 μg/mL catalase, and the indicated *N*-acylglycine (0.2−3.0 $K_{M,app}$). Initial rates were measured by following the α-AE-dependent consumption of O_2. V_M values were normalized to controls performed at 11.0 mM *N*-acetylglycine. [b] Kinetic constants ± standard error are from computer fits of the initial rate data to the Michaelis−Menten equation.

Table 2: Comparison of K_M, V_M, and V_M/K_M Values for *N*-Acylglycines with Rat α-AE in 2.5% (v/v) DMSO[a,b]

substrate	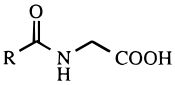	$K_{M,app}$ (mM)	$V_{M,app}$ (μmol min^{-1} mg^{-1})	relative $(V/K)_{app}$
N-acetylglycine	R = CH_3	$(1.5 \pm 0.14) \times 10^1$	7.5 ± 0.32	1.0
hippuric acid	R = C_6H_5	1.9 ± 0.059	8.3 ± 0.10	4.4
N-lauroylglycine	R = $CH_3(CH_2)_{10}$	0.11 ± 0.014	12.3 ± 0.78	220
N-myristoylglycine	R = $CH_3(CH_2)_{12}$	0.071 ± 0075	9.2 ± 0.50	260
N-oleoylglycine	R = $CH_3(CH_2)_7CH=CH(CH_2)_7$	0.094 ± 0.034	17.7 ± 3.8	380
N-linolenoylglycine	R = $CH_3CH_2CH=CHCH_2CH=CHCH_2CH=CH(CH_2)_7$	0.069 ± 0.011	9.2 ± 0.94	270

[a] Reactions were carried out at 37 °C in 100 mM MES/NaOH, pH 6.0, 30 mM NaCl, 1.0% (v/v) ethanol, 0.001% (v/v) Triton X-100, 2.5% (v/v) DMSO, 5.0 mM sodium ascorbate, 1.0 μM $Cu(NO_3)_2$, 10 μg/mL catalase, and the indicated *N*-acylglycine (0.2−1.5K_M). Initial rates were measured by following the α-AE-dependent consumption of O_2. V_M values were normalized to controls performed at 8.3 mM *N*-acetylglycine. [b] Kinetic constants ± standard error are from computer fits of the initial rate data to the Michaelis−Menten equation.

adequately described by this simple model (eq 3). For this experiment, $[tBOC\text{-}glycine]_{initial}$ was in great excess over $[O_2]_{initial}$ and $[glyoxylate]_{final}$ was less than $[tBOC\text{-}glycine]_{initial}$. Glyoxylate production continued after the steady-state concentration of O_2 was ~0 but did not continue until the $[glyoxylate]_{final} = [N\text{-}acylglycine]_{initial}$, even upon prolonged incubation. A model that accounts for the dissolution of O_2 from the atmosphere and the ascorbate-mediated inactivation of α-AE (*57*) might describe the progress curves obtained when $[N\text{-}acylglycine]_{initial}$ is in excess of the $[O_2]_{initial}$. However, the conclusion that O_2 consumption is faster than glyoxylate production is clear from inspection of the progress curves during the interval of $[O_2]$ decreasing from 200 μM to ~0 (Figure 2A).

Characterization of the Intermediate Formed upon Amidation of N-Acylglycines. An HPLC method for the separation of *N*-butyrylglycine, *N*-butyryl-α-hydroxyglycine, and butyramide was developed to follow the progress of an *N*-butyrylglycine amidation reaction. Amidation of *N*-butyrylglycine results in the initial appearance of a compound that has the same retention time as synthetic (*R,S*)-*N*-butyryl-α-hydroxyglycine (Figure 3A). A second amidation reaction carried out in the presence of 100 μM *N*-Ac-Phe-pyruvate, a PAL-specific inhibitor with a $K_i = 0.24$ μM (*45*), results

Table 3: Comparison of $K_{i,s}$ Values Determined with Crude Human Serum α-AE and $K_{M,app}$ Values Determined with Purified Rat α-AE

N-acylglycine	$K_{i,s}$[a,b] (mM)	$K_{M,app}$ at pH 7.4[c] (mM)	$K_{M,app}$ at pH 6.0[d] (mM)
N-acetylglycine	6.9 ± 0.74	10 ± 0.53	9.3 ± 0.47
N-isovaleroylglycine	2.0 ± 0.14	3.8 ± 0.29	2.0 ± 0.13
N-tigloylglycine	7.9 ± 0.47	nd[e]	3.2 ± 0.20
N-lauroylglycine	0.17 ± 0.018	0.12 ± 0.014	0.061 ± 0.0031
N-oleoylglycine	0.36 ± 0.032	nd	0.094 ± 0.034

[a] Reactions were carried out at 37 °C in 50 mM HEPES/NaOH, pH 7.4, 1.2 mM ascorbate, 10 μM $Cu(NO_3)_2$, 60 μg/mL catalase, 4.0 μM *N*-dansyl-Tyr-Val-Gly, 6.1 mg/mL human serum, and the indicated *N*-acylglycine (0.4−$K_{i,s}$). Initial rates were measured by following the crude human serum α-AE-dependent amidation of *N*-dansyl-Tyr-Val-Gly by HPLC (*50*). Inhibition constants ± standard errors were determined by Dixon analysis. The $K_{M,app}$ value for *N*-dansyl-Tyr-Val-Gly employed in the calculation of the $K_{i,s}$ values was 3.5 ± 0.23 μM, determined at these reaction conditions with crude hs-α-AE. [b] Under these reaction conditions (pH 7.4), the specific activity of crude hs-α-AE is ∼400 000-fold lower than that of purified rat α-AE. [c] Reactions were carried out at 37 °C in 50 mM HEPES/NaOH, pH 7.4, 1.2 mM ascorbate, 1.0 μM $Cu(NO_3)_2$, 60 μg/mL catalase, 10−40 μg/mL rat α-AE, and the indicated *N*-acylglycine (0.4−10$K_{M,app}$). Initial rates were measured by following the rat α-AE-dependent consumption of O_2. Michealis constants ± standard error are from computer fits of the initial rate data to the Michaelis−Menten equation. [d] $K_{M,app}$ values are taken from Tables 1 and 2. The inhibition experiments were carried out at the optimal conditions described for crude human serum α-AE (*63*). The optimal conditions for purified rat α-AE are different (see legends to Tables 1 and 2). As a consequence, the $K_{M,app}$ values in the two columns differ, but only by a factor of ≤2. Crude hs-α-AE was virtually inactive at the pH 6.0 conditions shown to be optimum for purified rat α-AE (Merkler and Merkler, unpublished results). [e] nd, not determined.

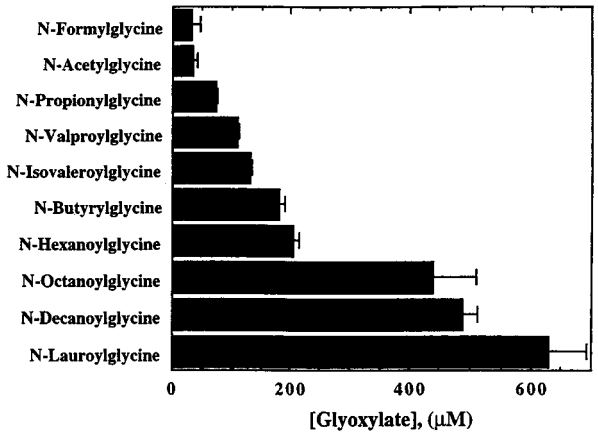

FIGURE 1: Glyoxylate production from 1.0 mM *N*-acylglycines. Reactions were initiated by the addition of 17 μg (0.23 nmol) of rat α-AE into 1.2 mL of 100 mM MES/NaOH, pH 6.0, 30 mM NaCl, 1.0% (v/v) ethanol, 0.001% (v/v) Triton X-100, 5.0 mM sodium ascorbate, 1.0 μM $Cu(NO_3)_2$, 10 μg/mL catalase, and 1.0 mM *N*-acylglycine. After 3 h at 37 °C, reactions were terminated by the addition of 200 μL of 6% (v/v) trifluoroacetic acid and glyoxylate was determined spectrophotometrically (see Materials and Methods). No glyoxylate was formed in controls lacking the *N*-acylglycine or α-AE. Error bars represent the standard deviation of four replicates.

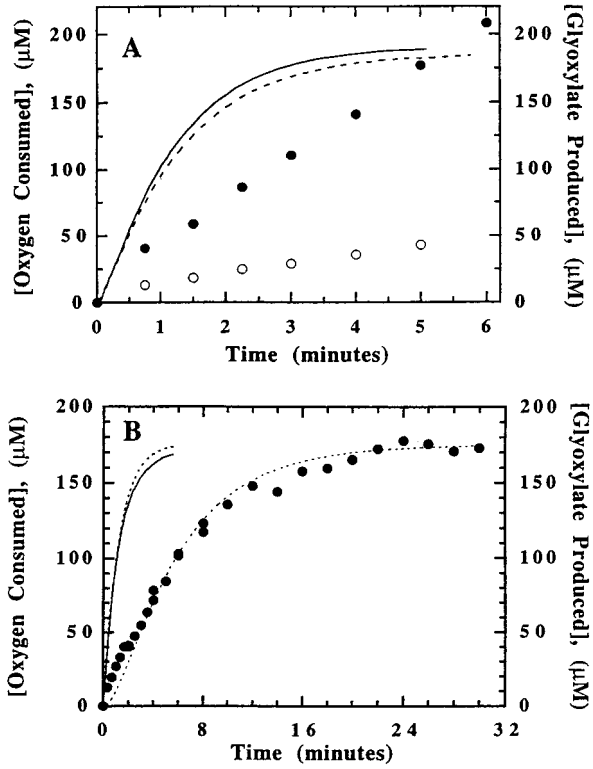

FIGURE 2: α-AE-Catalyzed consumption of O_2 (—) and the production of glyoxylate (●) from tBOC-glycine (A) and *N*-hexanoylglycine (B). Reactions at 37 °C were initiated by the addition of rat α-AE (106 μg, 1.4 nmol) to 3.0 mL of 100 mM MES/NaOH, pH 6.0, 30 mM NaCl, 1.0% (v/v) ethanol, 0.001% (v/v) Triton X-100, 5.0 mM sodium ascorbate, 1.0 μM $Cu(NO_3)_2$, 10 μg/mL catalase, and either 1.8 mM tBOC-glycine (A) or 180 μM *N*-hexanoylglycine (B). Progress curves for the consumption of O_2 (- - -) and the production of glyoxylate (○) from 1.8 mM tBOC-glycine in the presence of 15 μM *N*-Ac-Phe-pyruvate is also included in panel A. In panel B, the dotted lines (···) represent the fit to eqs 4−6 using $k_1 = 0.83$ min^{-1} and $k_2 = 0.19$ min^{-1}. In one sample, O_2 consumption was measured with an O_2 electrode. In a matched second sample, aliquots were removed at the indicated time and added to a vial containing one-fifth volume of 6% (v/v) TFA to quench the reaction. The concentration of glyoxylate in each quenched sample was determined spectrophotometrically.

in the accumulation of the species that coelutes with (*R*,*S*)-*N*-butyryl-α-hydroxyglycine and little formation of the butyramide (Figure 3B).

The data presented in Figure 3 strongly suggest that the formation of the acylamide from the *N*-acylglycine proceeds through a carbinolamide intermediate. The amidation of [*glycyl*-1,2-$^{13}C_2$]-tBOC-glycine was followed by $^1H-^{13}C$ HMQC NMR to unambiguously identify the intermediate as a carbinolamide. As tBOC-glycine is enzymatically converted first to tBOC-α-hydroxyglycine and ultimately to tBOC-amide by bifunctional α-AE, the ^{13}C NMR chemical shift of the α-glycyl carbon should change from an initial value of 43−45 ppm to 72−75 ppm for the carbinolamide intermediate and finally to 85−90 ppm for the α-carbon of glyoxylate (*58*). The amidation of [*glycyl*-1,2-$^{13}C_2$]-tBOC-glycine was followed by a two-dimensional NMR technique to ensure that the ^{13}C shift of the α-carbon of the intermediate was well-resolved from those of the MES buffer and ascorbate. The HMQC spectrum of the α-carbon of [*glycyl*-1,2-$^{13}C_2$]-tBOC-glycine is shown in Figure 4A, of the compound that accumulates upon the amidation of [*glycyl*-1,2-$^{13}C_2$]-tBOC-glycine in the presence of 100 μM *N*-Ac-

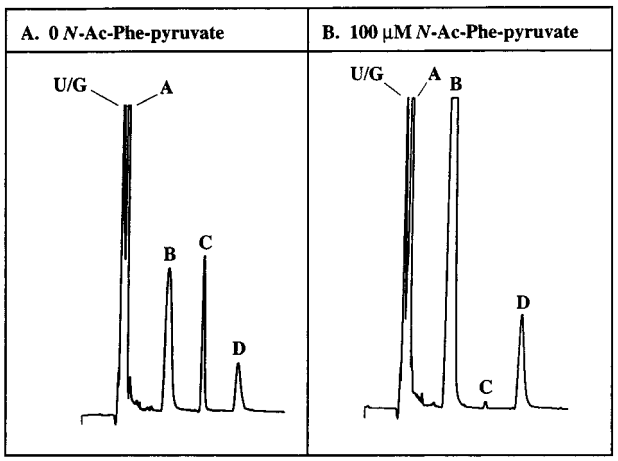

FIGURE 3: Amidation of *N*-butyrylglycine in the absence (A) or presence (B) of *N*-Ac-Phe-pyruvate. Reactions at 37 °C were initiated by the addition of rat α-AE (43 μg, 0.57 nmol) to 0.6 mL of 100 mM MES/NaOH, pH 6.0, 30 mM NaCl, 1.0% (v/v) ethanol, 0.001% (v/v) Triton X-100, 5.0 mM sodium ascorbate, 1.0 μM $Cu(NO_3)_2$, 10 μg/mL catalase, 4.0 mM *N*-butyrylglycine, and either 0 (A) or 100 μM *N*-Ac-Phe-pyruvate (B). After a 280 min incubation, a 25 μL aliquot of the reaction mixture was analyzed by HPLC as described in the Materials and Methods section. The peaks have the same retention times as standards added to reaction mix without enzyme: U/G = unknown/glyoxylate, A = reaction mix components, B = *N*-butyryl-α-hydroxyglycine, C = butyramide, and D = *N*-butyrylglycine. At time = 0, the controls without α-AE show only peaks A (reaction mix components) and D (*N*-butyrylglycine) (not shown). At time = 280 min, a peak that coelutes with glyoxylate is present in the controls. This is probably a byproduct of the Fenton chemistry between ascorbate and Cu(II).

Phe-pyruvate in Figure 4B, and of the α-carbon of [$^{13}C_2$]-glyoxylate that forms upon the amidation of [*glycyl*-1,2-$^{13}C_2$]-tBOC-glycine in the absence of *N*-Ac-Phe-pyruvate in Figure 4C. The spectrum shown in Figure 4B is completely consistent with the intermediate being *N*-(*tert*-butoxycarbanoyl)-α-hydroxyglycine. Incubation of *N*-hexanoylglycine with α-AE in the presence of 100 μM *N*-Ac-Phe-pyruvate resulted in the production of *N*-hexanoyl-α-hydroxyglycine, as confirmed by mass spectrometry with electrospray ionization (MS/ES+): *m*/*z* of 190.1 (M + H), 212.1 (M + Na), and 228.1 (M + K) (Figure S1, Supporting Information). *N*-Ac-Phe-pyruvate was absolutely essential to accumulating a sufficient concentration of the carbinolamide to characterize by NMR and mass spectrometry (see Figures 2A and 3B).

Inhibition of Human Serum PAM by N-(Fatty acyl)-glycines. The HPLC separation of *N*-dansyl-Tyr-Val-Gly from *N*-dansyl-Tyr-Val-NH_2 provides a sensitive assay for peptide amidation activity (*50*). Nonfluorescent substrates such as the *N*-fatty acylglycines can be treated as competitive inhibitors because their binding to α-AE will prevent the formation of *N*-dansyl-Tyr-Val-NH_2. As shown in Table 3, the *N*-(fatty acyl)glycines inhibit crude human serum α-AE (hs-α-AE). There is reasonable agreement between the $K_{i,s}$ values measured with hs-α-AE and the $K_{M,app}$ values measured with purified rat α-AE. The ratio of the $K_{i,s}/K_{M,app}$ ranges from 0.5 for *N*-isovaleroylglycine to ~3 for *N*-oleoylglycine (Table 3).[3] These results could represent species differences between the two enzymes used or the binding of the *N*-acylglycines to albumin in the crude serum. The binding of the *N*-(fatty acyl)glycines to hs-α-AE provides strong support for the pathway we have proposed for the biosynthesis of the fatty acid primary amides (Scheme 1).

DISCUSSION

α-*AE-Catalyzed Amidation of N-Acylglycines*. Merkler et al. (*20*) showed that α-AE converted *N*-myristoylglycine to myristamide. We show here for the first time that glyoxylate is also a product of *N*-acylgycine amidation (Figure 1). A comparison of the rate of O_2 consumption to the rate of glyoxylate production for *N*-acetylglycine, tBOC-glycine, *N*-hexanoylglycine, and *N*-oleoylglycine shows that O_2 is consumed faster than glyoxylate is formed (Figure 2). This result indicates that oxidation of the *N*-acylglycine does not lead directly to glyoxylate and the acylamide but first yields an oxidized intermediate. Our results from the amidation of *N*-butyrylglycine (Figure 3) and [*glycyl*-1,2-$^{13}C_2$]-tBOC-glycine (Figure 4) indicate that the oxidized intermediate is a carbinolamide, *N*-acyl-α-hydroxyglycine (Scheme 2). *N*-Acylglycine amidation is, thus, completely analogous to peptide amidation. The oxidative cleavage of glycine-extended peptides to α-amidated peptides and glyoxylate is a two-step reaction that proceeds via an α-hydroxyglycine-extended intermediate (*55*, *56*).

Relationship between N-Acylglycine Structure and $K_{M,app}$ Values. There is a 600−1000-fold variation in the $(V/K)_{app}$ values included in Tables 1 and 2. The variation in the $(V/K)_{app}$ is largely an effect on the $K_{M,app}$ because the $V_{M,app}$ varies less than 10-fold.[4] The length of the acyl chain is clearly an important determinant in the binding of the *N*-acylglycines to α-AE. The $K_{M,app}$ values decrease ~400-fold as the number of carbon atoms in the acyl chain increase from one (*N*-formylglycine, $K_{M,app} = 23 \pm 0.88$ mM) to 12 (*N*-lauroylglycine, $K_{M,app} = 61 \pm 3.1$ μM) (Table 1). As the number of carbon atoms in the acyl chain increases to >12, the $K_{M,app}$ value shows little change, remaining in the range of 60−90 μM (Table 2). Crystallographic studies show that PHM is composed of two domains that form a highly hydrophobic pocket (*59*). The substrate, *N*-α-Ac-(3,5-diiodotyrosyl)glycine, binds into the hydrophobic, interdomain cleft. The contribution to binding made by hydrophobic interactions between the *N*-acylglycines and PHM must be maximum for a straight-chain acyl moiety of 12 carbon atoms, i.e., *N*-lauroylglycine. Shorter-chain compounds (<12 carbon atoms) with fewer hydrophobic contacts exhibit higher $K_{M,app}$ values than *N*-lauroylglycine. Additional hydrophobic contacts possible with a longer-chain *N*-acylglycine (>12 carbon atoms) either are not made or are offset by other less favorable interactions with solvent or enzyme.

Replacement of the α- or β-carbon in the acyl chain with a nitrogen or an oxygen atom increases the $K_{M,app}$ ~3-fold. The ratio of the $K_{M,app}$ values for 5-butylhydantoic acid/*N*-hexanoylglycine is 2.9, for *N*-(methoxycarbonyl)glycine/*N*-propionylglycine is 2.6, for *N*-sarcosylglycine/*N*-butyryl-

[3] Mechanistic conclusions cannot be drawn from our data showing that the $K_{i,s}$ values ≈ the $K_{M,app}$ values. As discussed by Spector and Cleland (*85*), the $K_{i,s}$ value for an alternate substrate is equivalent to the $K_{M,app}$ value at the fixed concentrations of the other substrates.

[4] The variation in the $V_{M,app}$ is generally less than 2-fold. Only the $V_{M,app}$ values for *N*-(trifluoroacetyl)glycine and Gly-Gly are greater than 2-fold lower than the highest $V_{M,app}$ value measured, 12.6 μmol min^{-1} mg^{-1} for *N*-decanoylglycine.

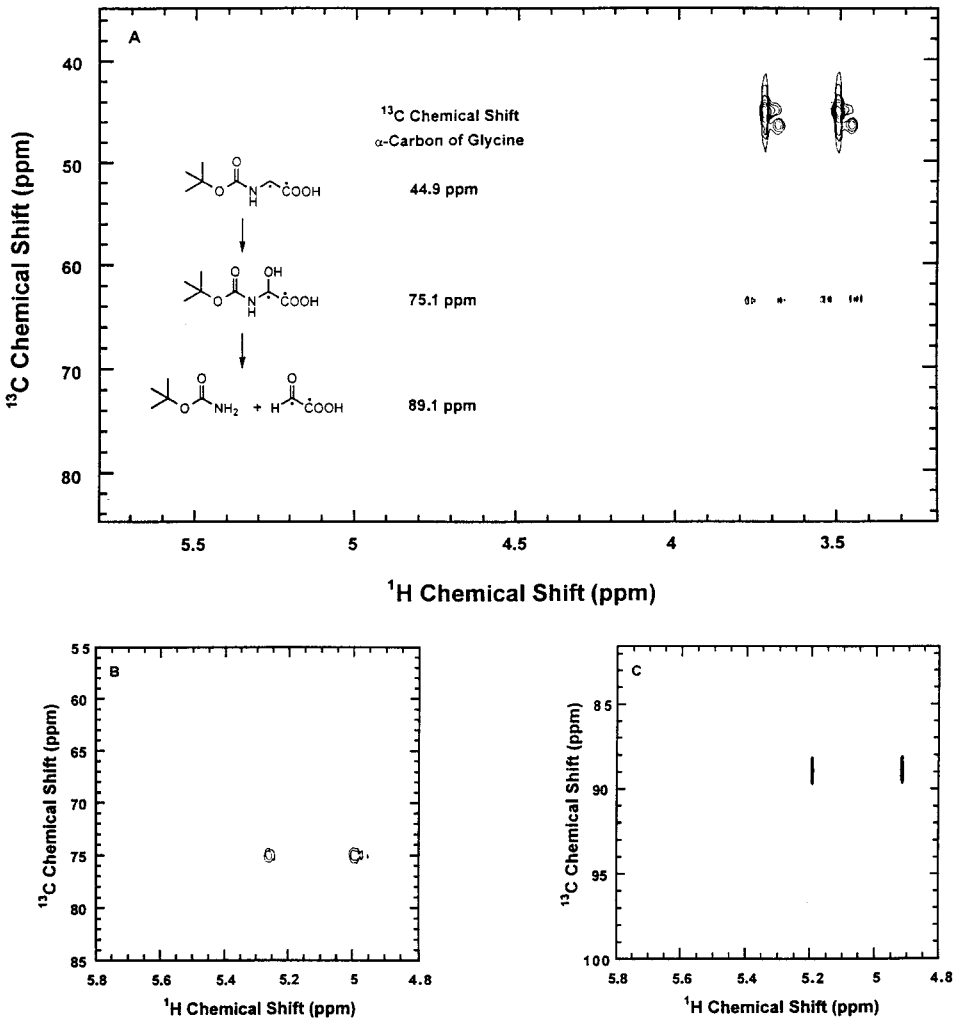

FIGURE 4: ^{1}H−^{13}C HMQC spectra of [*glycyl*-1,2-$^{13}C_2$]-tBOC-glycine (A), of [α-*hydroxyglycyl*-1,2-$^{13}C_2$]-tBOC-α-hydroxyglycine (B), and of [$^{13}C_2$]glyoxylate (C). Reactions were initiated by the addition of 260 μg (3.5 nmol) of α-AE into 1.6 mL of 10 mM MES/LiOD, pD 5.6, 4.0 mM NaCl, 7.0 mM sodium ascorbate, 1.0 μM $Cu(NO_3)_2$, 10 μg/mL catalase, 6.0 mM [*glycyl*-1,2-$^{13}C_2$]-tBOC-glycine, and 0 or 100 μM *N*-Ac-Phe-pyruvate. The final concentration of D_2O was 88% (v/v). Stock solutions of MES, NaCl, sodium ascorbate, and $Cu(NO_3)_2$ were prepared in D_2O. After a 3 h incubation at 37 °C, enzyme was removed prior to NMR analysis by diafiltration using a Centricon-30 filter. Panel A was obtained from a control without added α-AE, panel B from a reaction carried out in the presence of 100 μM *N*-Ac-Phe-pyruvate, and panel C from a reaction carried out in the absence of *N*-Ac-Phe-pyruvate. The resonances seen in panel A with ^{13}C chemical shifts of 63.3 and 63.6 ppm are from the reaction mix components and are present in the HMQC spectrum of a control sample lacking [*glycyl*-1,2-$^{13}C_2$]-tBOC-glycine. The spectra were acquired at 600 MHz at 27 °C and referenced to acetone as an external standard.

Scheme 2: α-AE-Catalyzed Amidation of *N*-Acylglycines

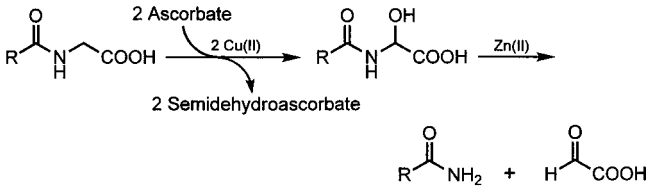

glycine is 2.9, and for hydantoic acid/*N*-acetylglycine is 3.5. The detrimental effect of an α- or β-oxygen or nitrogen in the acyl chain must result from a negative interaction with group(s) within the active site. The contact map of PHM with *N*-α-Ac-(3,5-diiodotyrosyl)glycine shows that M208 is located near the α- or β-position of the acyl chain (*59*). Perhaps a repulsive interaction between the sulfur atom of M208 and a nitrogen or oxygen at the α- or β-position of the acyl chain accounts for the small increase in $K_{M,app}$.

An α-AE-specific inhibitor could prove valuable in controlling the acute inflammatory response (*41*) and in treating certain cancers (*42*). Our discovery that α-AE amidates a diversity of *N*-acylglycines will likely stimulate the development of a clinically useful α-AE inhibitor. Soluble acylglycine analogues could first be designed with a short-chain acyl moiety (acetyl, propionyl, or butyryl group) and compared to our results with the corresponding *N*-acylglycine (Table 1). Once a lead compound is developed, a longer-chain acyl moiety could then be incorporated into second-generation compounds leading to a tight-binding, specific α-AE inhibitor. The limited aqueous solubility of a long-chain acyl inhibitor would not be a problem if the K_i value is sufficiently low. The cocrystalization of PHM with an *N*-acylglycine would provide considerable information concerning the interactions of enzyme with this class of substrates and is critical to utilizing the data reported here (Tables 1 and 2) in the design of a tight-binding, specific α-AE inhibitor.

Biosynthesis of Fatty Acid Primary Amides and Biological Significance of N-Acylglycine Amidation. Three different pathways have been proposed for the biosynthesis of the fatty acid amides: (a) the fatty acid amide hydrolyase-catalyzed

condensation of free fatty acids and ammonia (the reverse of the hydrolytic reaction) (*60*), (b) the aminolysis of phospholipids (*61*), and (c) the α-AE-catalyzed amidation of *N*-fatty acylglycines (*20*). The data presented here show that α-AE catalyzes the amidation of *N*-acylglycines in vitro in a reaction analogous to the peptide amidation reaction. There is evidence to suggest that *N*-acylglycine amidation to form the acylamides does occur in vivo.

Tissue distribution studies of ACGNAT in the Japanese monkey (*62*) and of α-AE in humans (*63*) co-localize the two enzymes in the cerebrum and the cerebellum.[5] The isolation of oleamide from the cerebrospinal fluid (CSF) of sleep-deprived cats (*3, 4*) suggests that oleamide and other fatty acid amides are produced in the brain and the CNS.

Another possibility for biosynthesis of the fatty acid amides is the amidation of hepatically derived *N*-acylglycines in blood by the α-AE found in the serum and plasma of humans (*63, 64*) and other mammals (*65, 66*). The liver is the major site of *N*-acylglycine biosynthesis. High levels of ACGNAT are found in the liver (*21, 22, 62*) and the acyl-CoA thioesters are collected in the liver as precursors to oxidative degradation (*67*). Numerous *N*-acylglycines have been identified in mammalian urine as a consequence of defects in fatty acid metabolism (*68*−*70*), electron transport (*71, 72*), or riboflavin biosynthesis (*73, 74*). Transport of the *N*-acyglycines from the liver into the blood is a necessary prerequisite for their urinary excretion. Evidence for the transport of the glycine conjugates from the liver to the blood include the accumulation of *N*-benzoylglycine (hippurate) in the blood following injection of benzoate into rats (*75*), the appearance of salicylurate (*o*-hydroxyhippurate) in the plasma after oral administration of aspirin (acetylsalicylate) to humans (*76, 77*), and the identification of *N*-isovaleroylglycine (*78*) and *N*-hexanoylglycine (*79*) in the blood of patients suffering from defects in fatty acid metabolism. After amidation of the hepatically derived *N*-acylglycines, the resulting acylamides could cross the blood−brain barrier to account for the presence of oleamide in the CSF. Blotnik et al. (*80*) have found that two acylamides, 2-*n*-propylpentanamide and 2-ethyl-3-methylpentanamide, cross the blood−brain barrier in rats. The isolation of five fatty acid amides from human plasma (*15*) and our inhibition data (Table 3) suggest that the fatty acid amides can be synthesized in the blood by α-AE. Note that the amidation of glycine-extended peptides in blood has also been postulated to account for the presence of α-amidated peptide hormones in tissues that do not contain α-AE (*81*).

α-AE is widely distributed throughout the body (*63*) and is involved in the biosynthesis of α-amidated peptides in the pituitary, the blood vessels, the epithelium of the lung, the α-cells of the pancreas, and gastrin-producing cells of the colon (*32, 81*). Similarly, the α-AE-dependent biosynthesis of the fatty acid amides could occur in more than one tissue. The potential role played by α-AE in the production of fatty acid amides in vivo is currently under investigation in our laboratories.

[5] Substrate specificity studies for ACGNAT are limited, focusing primarily on short chain acyl-CoA thioesters. Gregersen et al. (*86*) have shown that decanoyl-CoA is a substrate for human liver ACGNAT and we have found that lauroyl-CoA, palmitoyl-CoA, and oleoyl-CoA are substrates for bovine liver ACGNAT (Baumgart and Merkler, unpublished results).

The inhibition of peptide amidation by high levels of *N*-acylglycines could also be biologically significant. Dementia and other neurological problems associated with the organic acidemias (*82, 83*) might result from decreased levels of α-amidated neuropeptides. Low levels of α-AE activity in the brain and CSF have been correlated to Alzheimer's disease (*84*).

In conclusion, we have shown that bifunctional α-AE catalyzes the two-step conversion of *N*-fatty acylglycines to fatty acid primary amides and glyoxylate via a carbinolamide intermediate. The $(V/K)_{app}$ for the *N*-acylglycines increases as the acyl chain length increases such that the long-chain *N*-acylglycines exhibit $(V/K)_{app}$ values that are higher than that of D-Tyr-Val-Gly, a prototypical glycine-extended peptide substrate. The significance of these findings with regards to the design of novel α-AE inhibitors and the biosynthesis of fatty acid primary amides is discussed.

ACKNOWLEDGMENT

We thank Dr. James S. Phillips for a critical reading of the manuscript, Raviraj Kulathila for many helpful discussions, and Dr. Albin Otter for assistance with the HMQC NMR experiments.

SUPPORTING INFORMATION AVAILABLE

Synthetic procedures for compounds mentioned in the text and mass spectrum of enzymatically produced *N*-hexanoyl-α-hydroxyglycine. This material is available free of charge via the Internet at http://pubs.acs.org.

REFERENCES

1. Boger, D. L., Henrikson, S. J., and Cravatt, B. F. (1998) *Curr. Pharm. Des. 4*, 203−214.
2. Bezuglov, V. V., Bobrov, M. Yu., and Archakov, A. V. (1998) *Biochemistry (Moscow) 63*, 22−30.
3. Lerner, R. A., Siuzdak, G., Prospero-Garcia, O., Hendriksen, S. J., Boger, D. L., and Cravatt, B. F. (1994) *Proc. Natl. Acad. Sci. U.S.A. 91*, 9505−9508.
4. Cravatt, B. F., Prospero-Garcia, O., Siuzdak, G., Gilula, N. B., Henriksen, S. J., Boger, D. L., and Lerner, R. A. (1995) *Science 268*, 1506−1509.
5. Guan, X., Cravatt, B. F., Ehring, G. R., Hall, D. L., Boger, D. L., Lerner, R. A., and Gilula, N. B. (1997) *J. Cell Biol. 139*, 1785−1792.
6. Boger, D. L., Patterson, J. E., Guan, X., Cravatt, B. F., Lerner, R. A., and Guilula, N. B. (1998) *Proc. Natl. Acad. Sci. U.S.A. 95*, 4810−4815.
7. Huidobro-Toro, J. P., and Harris, R. A. (1996) *Proc. Natl. Acad. Sci. U.S.A. 93*, 8078−8082.
8. Thomas, E. A., Carson, M. J., Neal, M. J., and Sutcliffe, J. G. (1997) *Proc. Natl. Acad. Sci. U.S.A. 94*, 14115−14119.
9. Boger, D. L., Patterson, J. E., and Jin, Q. (1998) *Proc. Natl. Acad. Sci. U.S.A. 95*, 4102−4107.
10. Jain, M. K., Ghomashchi, F., Yu, B.-Z., Bayburt, T., Murphy, D., Houck, D., Brownell, J., Reid, J. C., Solowiej, J. E., Wong, S.-M., Mocek, U., Jarrell, R., Sasser, M., and Gelb, M. H. (1992) *J. Med. Chem. 35*, 3584−3586.
11. Mechoulam, R., Fride, E., Hanus, L., Sheskin, T., Bisogno, T., Di Marzo, V., Bayewitch, M., and Vogel, Z. (1997) *Nature 389*, 25−26.
12. Bisogno, T., Katayama, K., Melck, D., Ueda, N., De Petrocellis, L., Yamamoto, S., and Di Marzo, V. (1998) *Eur. J. Biochem. 254*, 634−642.
13. Wakamatsu, K., Masaki, T., Itoh, F., Kondo, K., and Sudo, K. (1990) *Biochem. Biophys. Res. Commun. 168*, 423−429.

14. Mitchell, C. A., Davies, M. J., Grounds, M. D., McGeachie, J. K., Crawford, G. J., Hong, Y., and Chirila, T. V. (1996) *J. Biomater. Appl. 10*, 230−249.
15. Arafat, E. S., Trimble, J. W., Andersen, R. N., Dass, C., and Desiderio, D. M. (1989) *Life Sci. 45*, 1679−1687.
16. Maurelli, S., Bisogno, T., De Petrocellis, L., Di Luccia, A., Marino, G., and Di Marzo, V. (1995) *FEBS Lett. 377*, 82−85.
17. Cravatt, B. F., Giang, D. K., Mayfield, S. P., Boger, D. L., Lerner, R. A., and Gilula, N. B. (1996) *Nature 384*, 83−87.
18. Giang, D. K., and Cravatt, B. F. (1997) *Proc. Natl. Acad. Sci. U.S.A. 94*, 2238−2242.
19. Thomas, E. A., Cravatt, B. F., Danielson, P. E., Gilula, N. B., and Sutcliffe, J. G. (1997) *J. Neurosci. Res. 50*, 1047−1052.
20. Merkler, D. J., Merkler, K. A., Stern, W., and Fleming, F. F. (1996) *Arch. Biochem. Biophys. 330*, 430−434.
21. Schachter, D., and Taggart, J. V. (1954) *J. Biol. Chem. 208*, 263−275.
22. Bartlett, K., and Gompertz, D. (1974) *Biochem. Med. 10*, 15−23.
23. Eipper, B. A., and Mains, R. E. (1988) *Annu. Rev. Physiol. 50*, 333−334.
24. Konopinska, D., Rosinski, G., and Sobótka, W. (1992) *Int. J. Pept. Protein Res. 39*, 1−11.
25. Schoofs, L., Veelaert, D., Vanden Broeck, J., and De Loof, A. (1997) *Peptides 18*, 145−156.
26. Bradbury, A. F., Finnie, M. D. A., and Smyth, D. G. (1982) *Nature 298*, 686−688.
27. Eipper, B. A., Mains, R. E., and Glembotski, C. C. (1983) *Proc. Natl. Acad. Sci. U.S.A. 80*, 5144−5148.
28. Kulathila, R., Consalvo, A. P., Fitzpatrick, P. F., Freeman, J. C., Snyder, L. M., Villafranca, J. J., and Merkler, D. J. (1994) *Arch. Biochem. Biophys. 311*, 191−195.
29. Bell, J., Ash, D. E., Snyder, L. M., Kulathila, R., Blackburn, N. J., and Merkler, D. J. (1997) *Biochemistry 36*, 16239−16246.
30. Klinman, J. P. (1996) *Chem. Rev. 96*, 2541−2561.
31. Kulathila, R., Merkler, K. A., and Merkler, D. J. (1999) *Nat. Prod. Rep. 16* (in press).
32. Eipper, B. A., Stoffers, D. A., and Mains, R. E. (1992) *Annu. Rev. Neurosci. 15*, 57−85.
33. Vos, M. D., Jones, J. E., and Treston, A. M. (1995) *Gene 163*, 307−311.
34. Kato, I., Yonekura, H., Yamamoto, H., and Okamoto, H. (1990) *FEBS Lett. 269*, 319−323.
35. Bertelsen, A. H., Beaudry, G. A., Galella, E. A., Jones, B. N., Ray, M. L., and Mehta, N. M. (1990) *Arch. Biochem. Biophys. 279*, 87−96.
36. Glauder, J., Ragg, H., Rauch, J., and Engels, J. W. (1990) *Biochem. Biophys. Res. Commun. 169*, 551−558.
37. Bradbury, A. F., and Smyth, D. G. (1983)*Biochem. Biophys. Res. Commun. 112*, 372−377.
38. Tamburini, P. P., Young, S. D., Jones, B. N., Palmesino, R. A., and Consalvo, A. P. (1990) *Int. J. Pept. Protein Res. 35*, 153−156.
39. Bradbury, A. F., and Smyth, D. G. (1987) *Eur. J. Biochem. 169*, 579−584.
40. Katopodis, A. G., and May, S. W. (1990) *Biochemistry 29*, 4541−4548.
41. Ogonowski, A. A., May, S. W., Moore, A. B., Barrett, L. T., O'Bryant, C. L., and Pollack, S. H. (1997) *J. Pharmacol. Exp. Ther. 280*, 846−853.
42. Treston, A. M., Scott, F. M., Vos, M., Iwai, N., Mains, R. E., Eipper, B. A., Cuttitta, F., and Mulshine, J. L. (1993) *Cell Growth Diff. 4*, 911−920.
43. Zoller, U., and Ben-Ishai, D. (1975) *Tetrahedron 31*, 863−866.
44. Roe, E. T., Scanlan, J. T., and Swern, D. (1949) *J. Am. Chem. Soc. 71*, 2215−2218.
45. Mounier, C. E., Shi, J., Sirimanne, S. R., Chen, B.-H., Moore, A. B., Gill-Woznichak, M. M., Ping, D., and May, S. W. (1997) *J. Biol. Chem. 272*, 5016−5023.
46. Katz, J., Liebermann, I., and Barker, H. A. (1953) *J. Biol. Chem. 200*, 431−441.
47. Davison, A. J., Kettle, A. J., and Fatur, D. J. (1986) *J. Biol. Chem. 261*, 1193−1200.
48. Matthews, D. E., Piparo, K. E., Burkett, V. H., and Pray, C. C. (1994) in *Animal Cell Technology: Products of Today, Prospects for Tomorrow* (Spier, R. E, Griffiths, J. B., and Bethold, W., Eds.) pp 315−319, Butterworth-Heinemann Ltd., Oxford, U.K.
49. Miller, D. A., Sayad, K. U., Kulathila, R., Beaudry, G. A., Merkler, D. J., and Bertelsen, A. H. (1992) *Arch. Biochem. Biophys. 298*, 380−388.
50. Jones, B. N., Tamburini, P. P., Consalvo, A. P., Young, S. D., Lovato, S. J., Gilligan, J. P., Jeng, A. Y., and Wennogle, L. P. (1988) *Anal. Biochem. 168*, 272−279.
51. Christman, A. A., Foster, P. W., and Esterer, M. B. (1944) *J. Biol. Chem. 155*, 161−171.
52. Matsui, M., Okada, M., and Ishidate, M. (1965) *Anal. Biochem. 12*, 143−149.
53. Cleland, W. W. (1979) *Methods Enzymol. 63*, 103−138.
54. Morrison, T. J., and Billett, F. (1952) *J. Chem. Soc.*, 3819−3822.
55. Young, S. D., and Tamburini, P. P. (1989) *J. Am. Chem. Soc. 111*, 1933−1934.
56. Katopodis, A. G., Ping, D., and May, S. W. (1990) *Biochemistry 29*, 6115−6120.
57. Merkler, D. J., Kulathila, R., Tamburini, P. P., and Young, S. D. (1992) *Arch. Biochem. Biophys. 294*, 594−602.
58. Pretsch, E., Seibl, J., and Simon, W. (1989) *Tables of Spectral Data for Structure Determination of Organic Compounds*, 2nd ed., pp C5−C265, Springer-Verlag, Berlin.
59. Prigge, S. T., Kolhekar, A. S., Eipper, B. A., Mains, R. E., and Amzel, L. M. (1997) *Science 278*, 1300−1305.
60. Sugiura, T., Kondo, S., Kodaka, T., Tonegawa, T., Nakane, S., Yamashita, A., Ishima, Y., and Waku, K. (1996) *Biochem. Mol. Biol. Int. 40*, 931−938.
61. Bisogno, T., Sepe, N., De Petrocellis, L., Mechoulam, R., and Di Marzo, V. (1997) *Biochem. Biophys. Res. Commun. 239*, 473−479.
62. Asaoka, K. (1991) *Int. J. Biochem. 23*, 429−434.
63. Wand, G. S., Ney, R. L., Baylin, S., Eipper, B. A., and Mains, R. E. (1985) *Metabolism 34*, 1044−1052.
64. Kapuscinski, M., Green, M., Sinha, S., Shepherd, J. J., and Shulkes, A. (1993) *Clin. Endocrinol. 39*, 51−58.
65. Eipper, B. A., Myers, A. C., and Mains, R. E. (1985) *Endocrinology 116*, 2497−2504.
66. Bolkenius, F. N., Ganzhorn, A. J., Chanal, M.-C., and Danzin, C. (1997) *Biochem. Pharmacol. 53*, 1695−1702.
67. Bremer, J., and Osmundsen, H. (1994) in *Fatty Acid Metabolism and Its Regulation* (Numa, S., Ed.) pp 113−154, Elsevier Science Publishers B. V., Amsterdam.
68. Vianey-Liaud, C., Divry, P., Gregersen, N., and Mathieu, M. (1987) *J. Inherited Metab. Dis. 10* (Suppl. 1), 159−198.
69. Bennett, M. J. (1990) *Ann. Clin. Biochem. 27*, 519−531.
70. Ozand, P. T., and Gascon, G. G. (1991) *J. Child Neurol. 6*, 196−219.
71. Lehnert, W., Wendel, U., Lindenmaier, S., and Böhm, N. (1982) *Eur. J. Pediatr. 139*, 56−59.
72. Shimizu, N., Yamaguchi, S., Orii, T., Previs, S. F., and Rinaldo, P. (1991) *Biol. Mass Spectrosc. 20*, 479−483.
73. Goodman, S. I. (1981) *Am. J. Clin. Nutr. 34*, 2434−2437.
74. Gregersen, N., and Kølvraa, S. (1982) *J. Inherited Metab. Dis. 5* (Suppl. 1), 17−18.
75. Gregus, Z., Fekete, T., Varga, F., and Klaassen, C. D. (1992) *Drug Metab. Dispos. 20*, 234−240.
76. Levy, G. (1965) *J. Pharm. Sci. 54*, 959−967.
77. Cham, B. E., Johns, D., Bochner, F., Imhoff, D. M., and Rowland, M. (1979) *Clin. Chem. 25*, 1420−1425.
78. de Sousa, C., Chalmers, R. A., Stacey, T. E., Tracey, B. M., Weaver, C. M., and Bradley, D. (1986) *Eur. J. Pediatr. 144*, 451−456.
79. Bennet, M. J., Ragni, M. C., Ostfeld, R. J., Santer, R., and Schmidt-Sommerfeld, E. (1994) *Ann. Clin. Biochem. 31*, 72−77.
80. Blotnik, S., Bergman, F., and Bialer, M. (1991) *Drug Metab. Dispos. 24*, 560−563.

81. Martínez, A., and Treston, A. M. (1996) *Mol. Cell. Endocrinol. 123*, 113−117.
82. Levy, H. L., and Erickson, A. M. (1974) in *Heritable Disorders of Amino Acid Metabolism: Patterns of Clinical Expression and Genetic Variation* (Nyhan, W. L., Ed.) pp 81−97, John Wiley, New York.
83. Sethi, K. D., Ray, R., Roesel, R. A., Carter, A. L., Gallagher, B. B., Loring, D. W., and Hommes, F. A. (1989) *Neurology 39*, 1343−1345.
84. Wand, G. S., May, C., May, V., Whitehouse, P. J., Rapoport, S. I., and Eipper, B. A. (1987) *Neurology 37*, 1057−1061.
85. Spector, T., and Cleland, W. W. (1981) *Biochem. Pharmacol. 30*, 1−7.
86. Gregersen, N., Kølvraa, S., and Mortensen, P. B. (1986) *Biochem. Med. Metab. Biol. 35*, 210−218.

BI982255J